THE JOURNAL OF PHYSICAL CHEMISTRY Letters

Letter

Cite This: J. Phys. Chem. Lett. 2018, 9, 2346−2352

pubs.acs.org/JPCL

# Reversible Hydrophobicity−Hydrophilicity Transition Modulated by Surface Curvature

Zhi Zhu,[†,∥] HongKai Guo,[‡,∥] XianKai Jiang,[†,∥] YongCong Chen,[§] Bo Song,[†] YiMing Zhu,*[,†] and SongLin Zhuang[†]

[†]Terahertz Technology Innovation Research Institute, Shanghai Key Lab of Modern Optical System, Terahertz Science Cooperative Innovation Center, School of Optical-Electrical Computer Engineering, University of Shanghai for Science and Technology, Shanghai 200093, PR China

[‡]Shijiazhuang Tiedao University, Shijiazhuang 050043, PR China

[§]Shanghai Center for Quantitative Life Sciences & Physics Department, Shanghai University, Shanghai 200444, PR China

Supporting Information

**ABSTRACT:** Wettability (hydrophobicity and hydrophilicity) is of fundamental importance in physical, chemical, and biological behaviors, resulting in widespread interest. Herein, by modulating surface curvature, we observed a reversible hydrophobic−hydrophilic transition on a model referred to a platinum surface. The underlying mechanism is revealed to be the competition between strong water−solid attraction and interfacial water orderliness. On the basis of the competition, we further propose an equation of wetting transition in the presence of an ordered interfacial liquid. It quantitatively reveals the relation of solid wettability with interfacial water orderliness and solid surface curvature, which can be used for predicting the critical point of the wetting transition. Our findings thus provide an innovative perspective on the design of a functional device demonstrating a reversible wettability transition and even a molecular-level understanding of biological functions.

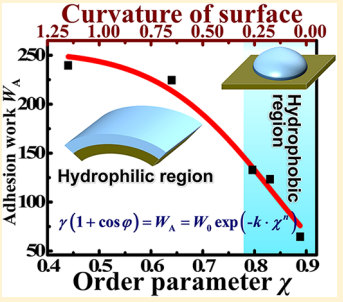


The wetting behavior of surfaces, as characterized by hydrophobicity (the material surface is seemingly repelled from a mass of water) and hydrophilicity (the material surface is attracted to water), has a fundamental bearing on various phenomena in physics,[1−5] chemistry,[6−9] and biology,[10,11] such as corrosion inhibition,[12−14] antifogging, surface drag reduction,[15−18] water permeation in membrane channels,[19,20] superhydrophobic surface coating,[6,21] and protein folding.[22−24]

The interaction between a solid surface and water is the key for understanding the wettability of a surface.[25,26] At room temperature, a hydrophobic characteristic has been observed on two different types of surfaces that are distinguished by the solid−water interaction. The first shows natural hydrophobicity due to weak interaction of the surface with water,[27] such as carbon-based,[28,29] $-CF_3$ terminated,[30] and $-CH_3$ terminated surfaces.[31] Especially, the surface of graphene, which has attracted intense interest for its wide potential applications,[32,33] has been proven both experimentally and theoretically to be hydrophobic with a contact angle of ∼87° between the water droplet and the surface.[28,34,35] The second type of surface shows interface-structure-induced hydrophobicity based on a strong attraction between the surface and water.[36,37] This hydrophobicity benefits from an ordered water layer at the solid−liquid interface and has been observed on many artificial and natural solid surfaces.[36−44] In 2009, Wang et al. constructed an artificial surface composed of a regular arrangement of positive and negative charges, which showed a hydrophobic characteristic induced by an ordered water layer.[36] In 2013, Limmer et al. observed that both the (100) and (111) surfaces of natural platinum (Pt) displayed interface-structure-induced hydrophobicity because the ordered interfacial water acted as a hydrophobic coating.[37,45] Moreover, it was reported both experimentally[46−50] and theoretically[37,38,49] that the hydrophobic Pt surface can support a droplet−surface contact angle of approximately 30°−50°. Similar hydrophobic phenomena have also been successively observed on the surfaces of several noble metals[38,40,41] (such as Pd, Cu, and Al), oxides[42] (such as $Al_2O_3$ and $SiO_2$), sapphire,[43] and talc.[44] Because the origin of the interface-structure-induced hydrophobicity is the ordered interfacial water, the hydrophobic characteristic of the surface should sensitively depend on the orderliness (i.e., geometric-structure regularity) of the interfacial water at the interface. Additionally, the orderliness is potentially associated with the defects,[5] temperature,[51] pressure, and even surface curvature. However, the roles of the last two terms on the wettability of a surface are little reported.

Surface curvature of nanostructures has been reported as able to be modulated by a mechanical stimulus (see the schematic representation shown in Figure 1),[52−56] especially the mechanosensitive porous media including endogenous protein channels[19,57,58] and synthetic analogues.[59,60] Perozo et al. showed that the channels in the cell membrane were sensitive to mechanical stimuli originating from membrane tension as

Received: March 11, 2018
Accepted: April 19, 2018
Published: April 19, 2018


© XXXX American Chemical Society

DOI: 10.1021/acs.jpclett.8b00749
J. Phys. Chem. Lett. 2018, 9, 2346−2352

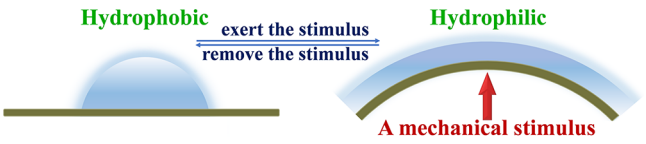


**Figure 1.** Schematic representation for the mechanical stimulus induced the change of curvature and the subsequent wetting transition. The brown and sky-blue layers represent the nanostructure and water, respectively. The red vector indicates the stimulus.

well as ions and other solutes.[56] Stevenson et al. observed the significant change of transmembrane-channel conformation driven by the stimuli.[61] Additionally, in biological systems, there is increasing observational evidence for the existence of ordered interfacial water.[62−65] Interestingly, it has been observed that the nanostructures exhibited a large variation in wettability linked to their geometry.[66]

Herein, through exploring the impact of solid-surface curvature on the wettability of solid, we propose a reversible hydrophobic−hydrophilic transition by modulating the curvature and subsequently an equation of this transition. Our molecular dynamics (MD) simulations showed that when the curvature was larger than 0.3 $nm^{-1}$, the hydrophobic characteristic of a model referred to the Pt surface disappeared and a hydrophilic behavior appeared. The underlying mechanism was revealed to be the competition of interfacial water orderliness and water−solid attraction. For revealing the quantitative relation of solid wettability with the interfacial water orderliness and solid surface curvature, we further proposed an equation of the wetting transition based on the competition above. This equation can be used to predict the critical curvature as well as critical orderliness of the wetting transition. These findings potentially provide a new perspective for understanding the functions of biological molecules and for designing functional materials and structures with a reversible wettability transition controlled by surface curvature and even by mechanical stimuli.

Pt(100) and graphene surfaces have been revealed to present interface-structure-induced[37,38] and natural[32−35] hydrophobicity, respectively. To explore the influence of surface curvature on wettability, two kinds of surface models referred to Pt(100) and graphene with different curvature were thus employed, denoted as Pt-surface and C-surface, respectively (see Figure 2a,b; details are provided in section 1 of the Supporting Information). Among the Pt-surface model, the Pt atom was characterized by the Lennard-Jones parameters with the potential well depth ($\varepsilon$) of 32.606 kJ/mol and the van der Waals radius ($\sigma$) of 2.53 Å.[38,67] The $\varepsilon$ of 0.2325 kJ/mol and the $\sigma$ of 3.4 Å were applied for a carbon (C) atom on the C-surface.[68,69] The water molecule was modeled by SPC/E.[70] The combining rules of the Lennard-Jones parameters for unlike atoms were geometric averages. The details of the simulation methods and corresponding discussion are provided in sections 2 and 3 of the Supporting Information. The critical contact angle of 90° was usually used to differentiate the hydrophobicity and hydrophilicity, but it contains more mathematical convenience than real physical and chemical meaning.[71] Notably, the surface of Pt metal was reported to be hydrophobic with a measured contact angle of 30°−50° of the droplet.[37,47] Moreover, the cosine value of the microscopic contact angle linearly relates to the droplet base curvature when it is calibrated to the macroscopic contact angle.[72] We thus applied the disappearance of the water droplet (i.e., the contact angle of the droplet was vanishing) as the transition point of wettability in our nanoscale simulations (the detailed discussion of transition point is in section 4 of the Supporting Information). After the MD simulations, further quantitative studies of the wetting transition were performed at a later stage that can apply to the transitions with a finite contact angle.

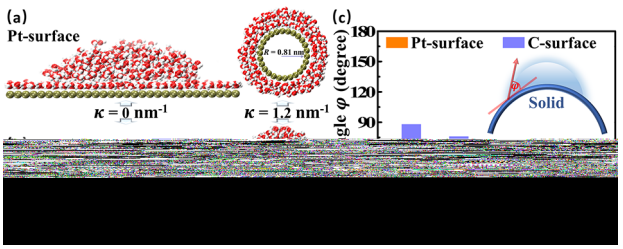


**Figure 2.** Typical conformations of dynamical equilibrium for the simulated systems and contact angles of water droplets for those conformations with different curvatures $\kappa$. The labels Pt-surface and C-surface indicate two surface models referred to Pt(100) and graphene, respectively. Typical conformations of dynamical equilibrium for water molecules on Pt-surface (a) and C-surface (b). (c) Contact angle $\varphi$ of water droplet residing on top of each conformation of Pt-surface (orange histogram) and C-surface (blue histogram). The inset is the schematic diagram of $\varphi$, where the red line and vector are the tangents of the surface and water droplet, respectively.

Our simulations showed that altering the surface curvature caused a wetting transition on the Pt-surface model. The typical conformations of dynamical equilibrium are presented in Figure 2a,b. For the Pt-surface, a stable water droplet coexists with a water monolayer on top of the surface for small curvature ($\kappa$ = 0 $nm^{-1}$) but not for large curvature ($\kappa$ = 1.2 $nm^{-1}$). In contrast, an obvious and stable water droplet resides upon the C-surface for both small ($\kappa$ = 0 $nm^{-1}$) and large ($\kappa$ = 1.2 $nm^{-1}$) curvatures. To characterize the surface wettability, we applied a contact angle ($\varphi$) for the water droplet residing on the surface, which is an intuitive and experimentally measurable physical quantity.[73,74] The $\varphi$ was calculated from the angle between the tangent at the contact point for the three-phase equilibrium profile of the water droplet and the corresponding tangent of the surface (the inset of Figure 2c; the details are provided in sections 5 and 6 of the Supporting Information). For the Pt-surface, $\varphi$ was approximately 51°, 30°, 10°, 0°, and 0° for $\kappa$ at 0, 0.2, 0.3, 0.6, and 1.2 $nm^{-1}$, respectively (Figure 2c). These results obviously indicate that as $\kappa$ increases, the wetting property of the Pt-surface changes from hydrophobic (when $\kappa \leq$ 0.3 $nm^{-1}$) to hydrophilic (when $\kappa >$ 0.3 $nm^{-1}$), corresponding to the gradual vanishing of the water droplet residing on the Pt-surface. In contrast, for the same changes in the C-surface curvature, the corresponding values of $\varphi$ were 88°, 76°, 67°, 62°, and 51°. Thus, the C-surface remains hydrophobic as $\kappa$ increases. We thus conclude that altering the surface curvature induces an essential change (i.e., hydrophobicity−hydrophilicity transition) on the wettability of the Pt-surface but not of the C-surface.

To understand the mechanism underlying the hydrophobicity−hydrophilicity transition of Pt-surface, we first investigated the curvature effect on the orderliness of water molecules in the first water layer ($H_2O$-first). The relative density distribution function of water molecules away from the surface was used to determine $H_2O$-first[69] (the details are in section 7 of the Supporting Information). The dipole distribution of water molecules was measured to describe the $H_2O$-first orderliness.[36] Two angles, $\alpha$ and $\beta$, were defined to


DOI: 10.1021/acs.jpclett.8b00749
J. Phys. Chem. Lett. 2018, 9, 2346−2352

characterize the dipole direction of a water molecule. $\alpha$ was the angle between the $x$-axis of the simulation box and the projection of the dipole onto the surface tangent, and $\beta$ was the angle between the dipole and the normal vector of the tangent plane (Figure 3, inset). The tangent plane crossed through the

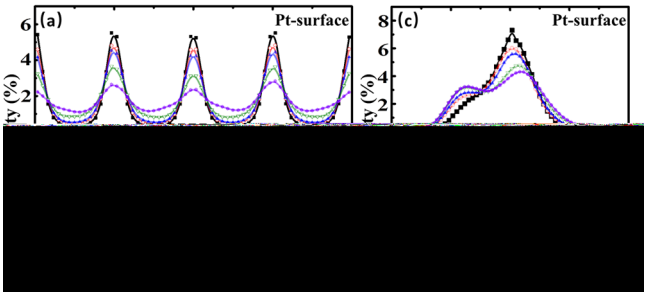


**Figure 3.** Effect of curvature ($\kappa$) on the dipole distribution of water molecules in the first layer on the models Pt-surface (a, c) and C-surface (b, d). The inset is a schematic diagram for directions $\alpha$ and $\beta$ of the dipole. The angle $\alpha$ is formed between the projection of the water dipole (orange vector) onto a surface tangent plane (gray trapezoid) and the $x$-axis (also the axial direction of tube for curved systems) of the simulation box (black vector). The angle $\beta$ is formed between the water dipole (red vector) and the normal vector (**W**) of the tangent plane (gray vector).

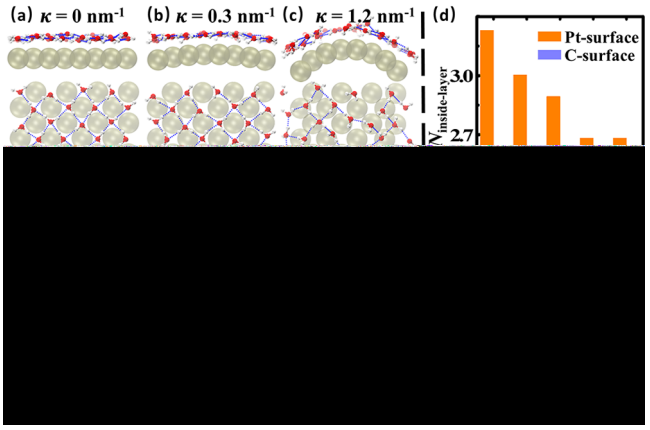


**Figure 4.** Curvature effect on H-bond networks. (a–c) Typical networks of H-bonds formed by the molecules of the first water layer on the models Pt-surface (upper) and C-surface (lower) with different curvature $\kappa$. The blue dashed line denotes the H-bond, and the tan and cyan spheres indicate platinum and carbon atoms of the surface models, respectively. (d) Average number of H-bonds per water molecule in the first water layer on the surface formed with other water molecules inside (upper) and outside (lower) the first layer. The orange and blue histograms represent the numbers for Pt-surface and C-surface, respectively.

mass center of the water molecule. The probability distribution of water dipoles with respect to $\alpha$ and $\beta$ were calculated. For the Pt-surface, the probability distribution of water dipoles with respect to $\alpha$ showed four peaks at 0°, 90°, 180°, and 270° for different $\kappa$ values (Figure 3a). The thickness of the Pt substrate has a weak effect on the results (the details are in section 8 of the Supporting Information). Notably, the height of these peaks decreased significantly as $\kappa$ increased, indicating that $H_2O$-first on the Pt-surface gradually became disordered as the curvature enhanced. In contrast, on the C-surface, the water–dipole probability distribution with respect to $\alpha$ was uniform (Figure 3b), meaning that $H_2O$-first remained disordered on the C-surface regardless of $\kappa$. Additionally, a single peak of probability distribution with respect to $\beta$ for different $\kappa$ values was observed at 90° of both the Pt-surface and C-surface (Figure 3c,d). However, the full width at half-maximum (fwhm) of the probability distribution of water dipoles on the Pt-surface with respect to $\beta$ was 17° for $\kappa$ at 0 $nm^{-1}$, 19° for $\kappa$ at 0.2 $nm^{-1}$, 28° for $\kappa$ at 0.3 $nm^{-1}$, 35° for $\kappa$ at 0.6 $nm^{-1}$, and 37° for $\kappa$ at 1.2 $nm^{-1}$. For the C-surface with various $\kappa$, the fwhm was almost unchanged with a value of 32°. These data imply that the average degree of dipoles aligned parallel to the surface tangent plane decreases as $\kappa$ increases for the Pt-surface but remains unchanged for the C-surface. Hence, we conclude that the alteration of surface curvature significantly changes the orderliness of $H_2O$-first on the Pt-surface, but not on the C-surface.

We then studied the curvature effect on the two-dimensional (2-D) network of hydrogen bonds (H-bonds, as closely related to water orderliness) in $H_2O$-first. Figure 4a–c shows the typical H-bond networks on the Pt-surface and C-surface with respect to $\kappa$ (the networks with all applied curvatures are presented in section 9 of the Supporting Information). For the Pt-surface with $\kappa$ = 0 $nm^{-1}$, the molecules of $H_2O$-first assembled into a 2-D structure and formed a H-bond network with rhombic patterns. This network led to each water molecule forming four H-bonds with neighboring water molecules within the $H_2O$-first. The molecules of $H_2O$-first were thus less able to form H-bonds with water molecules outside of this layer, resulting in the water droplet forming on the Pt-surface. As $\kappa$ increased, the regular 2-D H-bond network was gradually broken, which induced the molecules of $H_2O$-first to merge with the bulk water and caused the water droplet to disappear. In contrast, the curvature effects above did not occur on the C-surface, where the H-bond network of $H_2O$-first was always irregular.

We further explored the curvature effect on the H-bond number of $H_2O$-first. To estimate the formation of the H-bond between two water molecules, we adopted a conventional rule: oxygen distance $\leq$ 0.35 nm and H-bond angle < 30°.[10] The average numbers of H-bonds per molecule in $H_2O$-first under the droplet with the water molecules within ($N_{\text{inside-layer}}$) and outside ($N_{\text{outside-layer}}$) of the first layer were calculated. Upon $\kappa$ increase, $N_{\text{inside-layer}}$ decreased significantly from 3.23 to 2.68 on the Pt-surface, but it was almost unchanged with a value of 2.44 on the C-surface (Figure 4d). Besides these, $N_{\text{outside-layer}}$ increased significantly on the Pt-surface (from 0.43 to 0.81) but slightly on the C-surface (from 0.79 to 0.89). The increasing $\kappa$ of the Pt-surface thus causes the H-bond breaking between water molecules within the $H_2O$-first layer and then the H-bond forming between these water molecules and those outside of the layer. Therefore, the curvature of the Pt-surface but not the C-surface significantly affects the bonding preference of the molecules of $H_2O$-first between molecules inside the layer and outside the layer.

We also investigated the curvature effect on the interaction of $H_2O$-first with a solid surface. The adsorption energy ($E_{\text{water–solid}}$) per water molecule on the surface was calculated based on the van der Waals interactions between the water molecule and all atoms of the surface. As the results in Table 1 show, for different curvatures, the adsorption strength $|E_{\text{water–solid}}|$ of the Pt-surface is far greater than the thermal fluctuation at room temperature $k_BT$ (~2.49 kJ/mol), but that of the C-surface is comparable to the $k_BT$. Therefore, a strong


DOI: 10.1021/acs.jpclett.8b00749
J. Phys. Chem. Lett. 2018, 9, 2346–2352

Table 1. Curvature Effect on the Interaction Energy per Water Molecule of $H_2O$-first with Solid Surface[a]

| curvature | 0.0 | 0.2 | 0.3 | 0.6 | 1.2 |
|---|---|---|---|---|---|
| Pt-surface | −21.2 ± 0.9 | −21.2 ± 1.4 | −21.1 ± 0.2 | −20.2 ± 2.4 | −17.7 ± 2.7 |
| C-surface | −4.6 ± 1.4 | −4.4 ± 0.2 | −4.8 ± 0.9 | −4.2 ± 1.4 | −3.9 ± 0.6 |

[a]The units are $nm^{-1}$ for the curvature and kJ/mol for the interaction.

attraction occurs for water molecules with the Pt-surface, distinguished from the weak attraction of the C-surface.

The wetting transition of Pt-surface thus can be attributed to the competition between two factors: (1) the $H_2O$-first orderliness and (2) the water−solid interaction. Specifically, as the curvature $\kappa$ is modulated from small to large, the orderliness of $H_2O$-first is changed from high to low (Figures 3 and 4), while the attraction strength of water and solid surface remains strong at approximately 20 kJ/mol (Table 1). For a small curvature, the high orderliness of $H_2O$-first dominates, resulting in the interface-structure-induced hydrophobicity of the surface. At the large curvature and the subsequently low orderliness of $H_2O$-first, the strong water−surface attraction dominates, resulting in the natural hydrophilicity of the surface. Hence, the wettability of the naturally hydrophilic surface sensitively depends on the surface curvature, implying that curvature can be used to effectively modulate a reversible hydrophilic−hydrophobic transition. Notably, there widely exist charges arranged on biological interfaces, which could cause the formation of ordered interfacial water[62−65,75] (the curvature effect on the wetting of charged surface is shown in section 10 of the Supporting Information). The revealed mechanism above thus would apply generally, not just to the Pt-surface.

Finally, we studied the quantitative relation of liquid droplet contact angle with the interfacial water orderliness, solid surface curvature, and liquid−solid interaction and then revealed an equation of the curvature-modulated wetting transition based on the previous orderliness−interaction competition. Conventionally, there is the Young−Dupré equation for wetting transition, involving adhesion work ($W_A$) per unit area, contact angle ($\varphi$), and surface tension ($\gamma$), i.e. $\gamma(1 + \cos\varphi) = W_A$.[72,76] There, the work ($W_A$) is applied for the liquid−solid interaction, while the tension ($\gamma$) is 73.6 $mJ/m^2$ for water by the SPC/E model.[77] However, the above equation does not take the effect of interfacial liquid orderliness into account. To quantify the orderliness of $H_2O$-first on the Pt-surface, we introduced an order parameter $\chi = (P_{max} - P_{min})/(P_{max} + P_{min})$, where $P_{max}$ and $P_{min}$ are the maximum and minimum (Figure 3a) of probability in the dipole distribution with respect to $\alpha$. The values of $\chi$ were 0.89, 0.83, 0.80, 0.64, and 0.44 when $\kappa$ = 0, 0.2, 0.3, 0.6, and 1.2 $nm^{-1}$, respectively, indicating a linear relation of the orderliness and curvature, $\chi = b\kappa + c$, with $b$ = −0.39 ± 0.02 nm and $c$ = 0.90 ± 0.01 (Figure 5a). We then calculated $W_A$ of the interfacial water on the Pt-surface for various $\chi$ based on the interaction energy of water molecules and the Pt-surface[76,78−80] (the details are provided in section 11 of the Supporting Information). The values of $W_A$ were 64.59, 123.36, 132.90, 224.53, and 239.65 $mJ/m^2$ corresponding to $\chi$ = 0.89, 0.83, 0.80, 0.64, and 0.44, respectively (Figure 5b). Fitting the data above, we found an exponential relation of the adhesion work and orderliness, $W_A = W_0 \exp(-k\chi^n)$, with $W_0$ = 253.03 ± 10.16 $mJ/m^2$, $k$ = 2.45 ± 0.24, and $n$ = 6. By combination of the Young−Dupré formula, an equation of interfacial liquid orderliness and solid wettability was thus discovered:

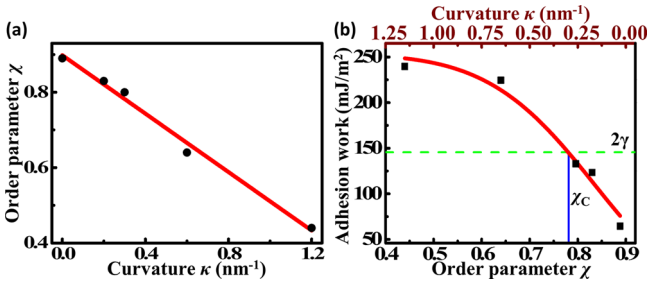


Figure 5. Relation of the Pt-surface curvature ($\kappa$), $H_2O$-first order parameter ($\chi$), and adhesion work per unit area ($W_A$) of the interfacial water. (a) Dependence of $\chi$ on $\kappa$ (black dots), fitted by the red line. (b) Dependence of $W_A$ on $\chi$ (black squares), fitted by the red curve. The blue line denotes the critical order $\chi_C$ of 0.78 upon $W_A = 2\gamma$ (green dashed line).

$$\gamma(1 + \cos\varphi) = W_0 \exp(-k\chi^n) \quad (1)$$

where $W_0$ indicates the adhesion work of the disordered interfacial liquid and solid; $k$ denotes the effect rate of interfacial liquid order, and $n$ means the power index of the order parameter $\chi$. For the case of water on the Pt-surface model, eq 1 gave a critical order $\chi_C$ = 0.78 at $\varphi$ = 0, i.e., the transition point of hydrophobicity and hydrophilicity. With help of the $\kappa$ and $\chi$ relation (Figure 5a), we then got critical curvature $\kappa_C$ = 0.31 $nm^{-1}$, agreeing well with the previous MD observations of the Pt-surface (Figure 2c). Equation 1 thus can be used to determine the critical curvature of the wetting transition when the tension of the liquid surface, the adhesion work of the disordered interfacial liquid, and the relation of the solid curvature and interfacial liquid orderliness are given. It is worth noting that this equation can also apply to the case of wetting transitions with a finite contact angle.

In summary, by modulating surface curvature, we found a reversible transition between hydrophobicity and hydrophilicity on the Pt-surface model but not on the C-surface model. The difference of surface behaviors was attributed to the fact that the naturally hydrophilic Pt-surface presented interface-structure-induced hydrophobicity at small curvature, while the C-surface always remained naturally hydrophobic. Specifically, the hydrophobicity of the Pt-surface was caused by the existence of interfacial ordered water, and the hydrophobicity of the C-surface was due to the weak attraction between the water and surface. Therefore, as the surface curvature increased, the orderliness and 2-D H-bond network in the interfacial water layer on the Pt-surface were significantly disrupted, causing the disappearance of the interface-structure-induced hydrophobicity. In contrast, the curvature change cannot affect the weak attraction between the water and the C-surface, and thus the surface remained hydrophobic. On the basis of the physics above of water on the Pt-surface model, we further proposed an equation of the wetting transition in the presence of an ordered interfacial liquid by improving Young's equation. The improved equation reveals the quantitative relation of solid wettability with interfacial water orderliness and solid surface curvature and can be used for predicting the critical orderliness and



DOI: 10.1021/acs.jpclett.8b00749
J. Phys. Chem. Lett. 2018, 9, 2346−2352

curvature of the wetting transition. Remarkably, the surface curvature of nanostructures involving biological systems could be modulated by mechanical stimuli. Therefore, our findings show potential for the development of device and material designs for the realization of a controllable hydrophobicity−hydrophilicity transition and even for the understanding of biomolecular functions.

## ■ ASSOCIATED CONTENT

### Supporting Information

The Supporting Information is available free of charge on the ACS Publications website at DOI: 10.1021/acs.jpclett.8b00749.

Conformations of simulated systems; methods of simulations; discussion of the applied force fields; definition of surface hydrophobicity; methods of contact angle measurement; methods for determining stability of contact angle; density distribution functions of water molecules on different surfaces; thickness effect of substrate on interfacial water molecules; full typical results of H-bond networks; curvature effect on the wetting of a charged surface; calculation method of adhesion work (PDF)

## ■ AUTHOR INFORMATION


### Corresponding Author

*E-mail: ymzhu@usst.edu.cn.

### ORCID

Bo Song: 0000-0001-5600-106X


### Author Contributions

‖Z.Z., H.G., and X.J. contributed equally to this work.

### Notes

The authors declare no competing financial interest.

## ■ ACKNOWLEDGMENTS

This work was supported by the National Program on Key Basic Research Project of China (973 Program) (2014CB339806), the Major National Development Project of Scientific Instrument and Equipment (2017YFF0106300, 2016YFF0100503), the National Natural Science Foundation of China (61722111, 61771314), the Key Scientific and Technological Project of Science and Technology Commission of Shanghai Municipality (15DZ0500102), Shanghai leading talent (2016-019), and Young Yangtse River Scholar (Q2016212).

## ■ REFERENCES


(1) Hummer, G.; Garde, S. Cavity Expulsion and Weak Dewetting of Hydrophobic Solutes in Water. *Phys. Rev. Lett.* **1998**, *80*, 4193.

(2) Meng, S.; Zhang, Z.; Kaxiras, E. Tuning Solid Surfaces from Hydrophobic to Superhydrophilic by Submonolayer Surface Modification. *Phys. Rev. Lett.* **2006**, *97*, 036107.

(3) Yuan, Q.; Zhao, Y. P. Precursor Film in Dynamic Wetting, Electrowetting, and Electro-elasto-capillarity. *Phys. Rev. Lett.* **2010**, *104*, 246101.

(4) Hu, G. H.; Xu, A. J.; Xu, Z.; Zhou, Z. W. Dewetting of Nanometer Thin Films under an Electric Field. *Phys. Fluids* **2008**, *20*, 102101.

(5) Wang, C.; Zhou, B.; Xiu, P.; Fang, H. Effect of Surface Morphology on the Ordered Water Layer at Room Temperature. *J. Phys. Chem. C* **2011**, *115*, 3018−3024.

(6) Genzer, J.; Efimenko, K. Creating Long-lived Superhydrophobic Polymer Surfaces through Mechanically Assembled Monolayers. *Science* **2000**, *290*, 2130−2133.

(7) Scatena, L.; Brown, M.; Richmond, G. Water at Hydrophobic Surfaces: Weak Hydrogen Bonding and Strong Orientation Effects. *Science* **2001**, *292*, 908−912.

(8) Meng, S.; Xu, L. F.; Wang, E. G.; Gao, S. Vibrational Recognition of Hydrogen-bonded Water Networks on a Metal Surface. *Phys. Rev. Lett.* **2002**, *89*, 176104.

(9) Xiu, P.; Zhou, B.; Qi, W.; Lu, H.; Tu, Y.; Fang, H. Manipulating Biomolecules with Aqueous Liquids Confined within Single-walled Nanotubes. *J. Am. Chem. Soc.* **2009**, *131*, 2840−2845.

(10) Hummer, G.; Rasaiah, J. C.; Noworyta, J. P. Water Conduction through the Hydrophobic Channel of a Carbon Nanotube. *Nature* **2001**, *414*, 188−190.

(11) Zhou, R.; Huang, X.; Margulis, C. J.; Berne, B. J. Hydrophobic Collapse in Multidomain Protein Folding. *Science* **2004**, *305*, 1605−1609.

(12) Yin, Y.; Liu, T.; Chen, S.; Liu, T.; Cheng, S. Structure Stability and Corrosion Inhibition of Super-hydrophobic Film on Aluminum in Seawater. *Appl. Surf. Sci.* **2008**, *255*, 2978−2984.

(13) Wang, P.; Zhang, D.; Qiu, R.; Hou, B. Super-hydrophobic Film Prepared on Zinc as Corrosion Barrier. *Corros. Sci.* **2011**, *53*, 2080−2086.

(14) Maeztu, J. D.; Rivero, P. J.; Berlanga, C.; Bastidas, D. M.; Palacio, J. F.; Rodriguez, R. Effect of Graphene Oxide and Fluorinated Polymeric Chains Incorporated in a Multilayered Sol-gel Nanocoating for the Design of Corrosion Resistant and Hydrophobic Surfaces. *Appl. Surf. Sci.* **2017**, *419*, 138−149.

(15) Quéré, D. Non-sticking Drops. *Rep. Prog. Phys.* **2005**, *68*, 2495.

(16) Zhang, X.; Shi, F.; Niu, J.; Jiang, Y.; Wang, Z. Superhydrophobic Surfaces: From Structural Control to Functional Application. *J. Mater. Chem.* **2008**, *18*, 621−633.

(17) Li, X. M.; Reinhoudt, D.; Crego-Calama, M. What do We Need for a Superhydrophobic Surface? A Review on the Recent Progress in the Preparation of Superhydrophobic Surfaces. *Chem. Soc. Rev.* **2007**, *36*, 1350−1368.

(18) Wang, C.; Wen, B.; Tu, Y.; Wan, R.; Fang, H. Friction Reduction at a Superhydrophilic Surface: Role of Ordered Water. *J. Phys. Chem. C* **2015**, *119*, 11679−11684.

(19) de Groot, B. L.; Grubmüller, H. Water Permeation across Biological Membranes: Mechanism and Dynamics of Aquaporin-1 and GlpF. *Science* **2001**, *294*, 2353−2357.

(20) Beckstein, O.; Sansom, M. S. Liquid−vapor Oscillations of Water in Hydrophobic Nanopores. *Proc. Natl. Acad. Sci. U. S. A.* **2003**, *100*, 7063−7068.

(21) Erbil, H. Y.; Demirel, A. L.; Avcı, Y.; Mert, O. Transformation of a Simple Plastic into a Superhydrophobic Surface. *Science* **2003**, *299*, 1377−1380.

(22) Brooks, C. L.; Gruebele, M.; Onuchic, J. N.; Wolynes, P. G. Chemical Physics of Protein Folding. *Proc. Natl. Acad. Sci. U. S. A.* **1998**, *95*, 11037−11038.

(23) Dobson, C. M.; Šali, A.; Karplus, M. Protein Folding: A Perspective from Theory and Experiment. *Angew. Chem., Int. Ed.* **1998**, *37*, 868−893.

(24) Brooks, C. L.; Onuchic, J. N.; Wales, D. J. Taking a Walk on a Landscape. *Science* **2001**, *293*, 612−613.

(25) Björneholm, O.; Hansen, M. H.; Hodgson, A.; Liu, L. M.; Limmer, D. T.; Michaelides, A.; Pedevilla, P.; Rossmeisl, J.; Shen, H.; Tocci, G.; et al. Water at Interfaces. *Chem. Rev.* **2016**, *116*, 7698−7726.

(26) Liu, K.; Jiang, L. Metallic Surfaces with Special Wettability. *Nanoscale* **2011**, *3*, 825−838.

(27) Shen, Y. R.; Ostroverkhov, V. Sum-frequency Vibrational Spectroscopy on Water Interfaces: Polar Orientation of Water Molecules at Interfaces. *Chem. Rev.* **2006**, *106*, 1140−1154.

(28) Li, H.; Zeng, X. C. Wetting and Interfacial Properties of Water Nanodroplets in Contact with Graphene and Monolayer Boron−nitride Sheets. *ACS Nano* **2012**, *6*, 2401−2409.

(29) Falk, K.; Sedlmeier, F.; Joly, L.; Netz, R. R.; Bocquet, L. Molecular Origin of Fast Water Transport in Carbon Nanotube Membranes: Superlubricity versus Curvature Dependent Friction. *Nano Lett.* **2010**, *10*, 4067−4073.




DOI: 10.1021/acs.jpclett.8b00749
*J. Phys. Chem. Lett.* 2018, 9, 2346−2352

(30) Granick, S.; Bae, S. C. A Curious Antipathy for Water. *Science* **2008**, *322*, 1477−1478.
(31) Poynor, A.; Hong, L.; Robinson, I. K.; Granick, S.; Zhang, Z.; Fenter, P. A. How Water Meets a Hydrophobic Surface. *Phys. Rev. Lett.* **2006**, *97*, 266101.
(32) Suk, M. E.; Aluru, N. Water Transport through Ultrathin Graphene. *J. Phys. Chem. Lett.* **2010**, *1*, 1590−1594.
(33) Raj, R.; Maroo, S. C.; Wang, E. N. Wettability of Graphene. *Nano Lett.* **2013**, *13*, 1509−1515.
(34) Taherian, F.; Marcon, V.; van der Vegt, N. F.; Leroy, F. What is the Contact Angle of Water on Graphene? *Langmuir* **2013**, *29*, 1457−1465.
(35) Annamalai, M.; Gopinadhan, K.; Han, S. A.; Saha, S.; Park, H. J.; Cho, E. B.; Kumar, B.; Patra, A.; Kim, S. W.; Venkatesan, T. Surface Energy and Wettability of Van der Waals Structures. *Nanoscale* **2016**, *8*, 5764−5770.
(36) Wang, C.; Lu, H.; Wang, Z.; Xiu, P.; Zhou, B.; Zuo, G.; Wan, R.; Hu, J.; Fang, H. Stable Liquid Water Droplet on a Water Monolayer Formed at Room Temperature on Ionic Model Substrates. *Phys. Rev. Lett.* **2009**, *103*, 137801.
(37) Limmer, D. T.; Willard, A. P.; Madden, P.; Chandler, D. Hydration of Metal Surfaces can be Dynamically Heterogeneous and Hydrophobic. *Proc. Natl. Acad. Sci. U. S. A.* **2013**, *110*, 4200−4205.
(38) Xu, Z.; Gao, Y.; Wang, C.; Fang, H. Nanoscale Hydrophilicity on Metal Surfaces at Room Temperature: Coupling Lattice Constants and Crystal Faces. *J. Phys. Chem. C* **2015**, *119*, 20409−20415.
(39) Ball, P. How Wet can You Get? *Nat. Phys.* **2016**, *12*, 718−718.
(40) Michaelides, A.; Morgenstern, K. Ice Nanoclusters at Hydrophobic Metal Surfaces. *Nat. Mater.* **2007**, *6*, 597−601.
(41) Pedroza, L. S.; Poissier, A.; Fernández-Serra, M. V. Local Order of Liquid Water at Metallic Electrode Surfaces. *J. Chem. Phys.* **2015**, *142*, 034706.
(42) Phan, A.; Ho, T. A.; Cole, D.; Striolo, A. Molecular Structure and Dynamics in Thin Water Films at Metal Oxide Surfaces: Magnesium, Aluminum, and Silicon Oxide Surfaces. *J. Phys. Chem. C* **2012**, *116*, 15962−15973.
(43) Lützenkirchen, J.; Zimmermann, R.; Preočanin, T.; Filby, A.; Kupcik, T.; Küttner, D.; Abdelmonem, A.; Schild, D.; Rabung, T.; Plaschke, M.; et al. An Attempt to Explain Bimodal Behaviour of the Sapphire C-plane Electrolyte Interface. *Adv. Colloid Interface Sci.* **2010**, *157*, 61−74.
(44) Rotenberg, B.; Patel, A. J.; Chandler, D. Molecular Explanation for Why Talc Surfaces can be both Hydrophilic and Hydrophobic. *J. Am. Chem. Soc.* **2011**, *133*, 20521−20527.
(45) Limmer, D. T.; Willard, A. P.; Madden, P. A.; Chandler, D. Water Exchange at a Hydrated Platinum Electrode is Rare and Collective. *J. Phys. Chem. C* **2015**, *119*, 24016−24024.
(46) Bewig, K.; Zisman, W. The Wetting of Gold and Platinum by Water. *J. Phys. Chem.* **1965**, *69*, 4238−4242.
(47) Xu, Y.; Dibble, C. J.; Petrik, N. G.; Smith, R. S.; Kay, B. D.; Kimmel, G. A. Complete Wetting of Pt(111) by Nanoscale Liquid Water Films. *J. Phys. Chem. Lett.* **2016**, *7*, 541−547.
(48) Erb, R. A. Wettability of Metals under Continuous Condensing Conditions. *J. Phys. Chem.* **1965**, *69*, 1306−1309.
(49) Kandlikar, S. G.; Steinke, M. E.; Maruyama, S.; Kimura, T. Molecular Dynamics Simulation and Measurement of Contact Angle of Water Droplet on a Platinum Surface. In *Proceedings of 2001 ASME IMECE*; New York, 2001; pp 343−348.
(50) Kimmel, G. A.; Petrik, N. G.; Dohnálek, Z.; Kay, B. D. Crystalline Ice Growth on Pt(111): Observation of a Hydrophobic Water Monolayer. *Phys. Rev. Lett.* **2005**, *95*, 166102.
(51) Cheh, J.; Gao, Y.; Wang, C.; Zhao, H.; Fang, H. Ice or Water: Thermal Properties of Monolayer Water Adsorbed on a Substrate. *J. Stat. Mech.: Theory Exp.* **2013**, *2013*, P06009.
(52) Bifano, T. G.; Johnson, H. T.; Bierden, P.; Mali, R. K. Elimination of Stress-induced Curvature in Thin-film Structures. *J. Microelectromech. Syst.* **2002**, *11*, 592−597.
(53) McMahon, H. T.; Gallop, J. L. Membrane Curvature and Mechanisms of Dynamic Cell Membrane Remodelling. *Nature* **2005**, *438*, 590−596.
(54) Zimmerberg, J.; Kozlov, M. M. How Proteins Produce Cellular Membrane Curvature. *Nat. Rev. Mol. Cell Biol.* **2006**, *7*, 9−19.
(55) Diz-Muñoz, A.; Fletcher, D. A.; Weiner, O. D. Use the Force: Membrane Tension as an Organizer of Cell Shape and Motility. *Trends Cell Biol.* **2013**, *23*, 47−53.
(56) Perozo, E.; Kloda, A.; Cortes, D. M.; Martinac, B. Physical Principles Underlying the Transduction of Bilayer Deformation Forces During Mechanosensitive Channel Gating. *Nat. Struct. Biol.* **2002**, *9*, 696−703.
(57) Murata, K.; Mitsuoka, K.; Hirai, T.; Walz, T.; Agre, P.; Heymann, J. B.; Engel, A.; Fujiyoshi, Y. Structural Determinants of Water Permeation through Aquaporin-1. *Nature* **2000**, *407*, 599−605.
(58) Zhou, Y. F.; Morais-Cabral, J. H.; Kaufman, A.; MacKinnon, R. Chemistry of Ion Coordination and Hydration Revealed by a $K^+$ channel-Fab Complex at 2.0 Angstrom Resolution. *Nature* **2001**, *414*, 43−48.
(59) Sakai, N.; Mareda, J.; Matile, S. Rigid-rod Molecules in Biomembrane Models: From Hydrogen-bonded Chains to Synthetic Multifunctional Pores. *Acc. Chem. Res.* **2005**, *38*, 79−87.
(60) Zhu, P. A.; Kong, T. T.; Tang, X.; Wang, L. Q. Well-defined Porous Membranes for Robust Omniphobic Surfaces via Microfluidic Emulsion Templating. *Nat. Commun.* **2017**, *8*, 15823.
(61) Stevenson, P.; Tokmakoff, A. Time-resolved Measurements of an Ion Channel Conformational Change Driven by a Membrane Phase Transition. *Proc. Natl. Acad. Sci. U. S. A.* **2017**, *114*, 10840−10845.
(62) Ruffle, S. V.; Michalarias, I.; Li, J. C.; Ford, R. C. Inelastic Incoherent Neutron Scattering Studies of Water Interacting with Biological Macromolecules. *J. Am. Chem. Soc.* **2002**, *124*, 565−569.
(63) Pal, S. K.; Zewail, A. H. Dynamics of Water in Biological Recognition. *Chem. Rev.* **2004**, *104*, 2099−2123.
(64) Chaplin, M. Opinion - Do We Underestimate the Importance of Water in Cell Biology? *Nat. Rev. Mol. Cell Biol.* **2006**, *7*, 861−866.
(65) Sommer, A. P.; Zhu, D.; Franke, R. P.; Fecht, H. J. Biomimetics: Learning from Diamonds. *J. Mater. Res.* **2008**, *23*, 3148−3152.
(66) Murison, J.; Semin, B.; Baret, J. C.; Herminghaus, S.; Schroter, M.; Brinkmann, M. Wetting Heterogeneities in Porous Media Control Flow Dissipation. *Phys. Rev. Appl.* **2014**, *2*, 034002.
(67) Heinz, H.; Vaia, R.; Farmer, B.; Naik, R. Accurate Simulation of Surfaces and Interfaces of Face-centered Cubic Metals Using 12−6 and 9−6 Lennard-Jones Potentials. *J. Phys. Chem. C* **2008**, *112*, 17281−17290.
(68) Koishi, T.; Yasuoka, K.; Fujikawa, S.; Ebisuzaki, T.; Zeng, X. C. Coexistence and Transition between Cassie and Wenzel State on Pillared Hydrophobic Surface. *Proc. Natl. Acad. Sci. U. S. A.* **2009**, *106*, 8435−8440.
(69) Qi, C.; Zhou, B.; Wang, C.; Zheng, Y.; Fang, H. A Nonmonotonic Dependence of the Contact Angles on the Surface Polarity for a Model Solid Surface. *Phys. Chem. Chem. Phys.* **2017**, *19*, 6665−6670.
(70) Berendsen, H.; Grigera, J.; Straatsma, T. The Missing Term in Effective Pair Potentials. *J. Phys. Chem.* **1987**, *91*, 6269−6271.
(71) Wang, S. T.; Song, Y. L.; Jiang, L. Photoresponsive surfaces with controllable wettability. *J. Photochem. Photobiol., C* **2007**, *8*, 18−29.
(72) Shih, C. J.; Wang, Q. H.; Lin, S. C.; Park, K. C.; Jin, Z.; Strano, M. S.; Blankschtein, D. Breakdown in the Wetting Transparency of Graphene. *Phys. Rev. Lett.* **2012**, *109*, 176101.
(73) Decker, E.; Frank, B.; Suo, Y.; Garoff, S. Physics of Contact Angle Measurement. *Colloids Surf., A* **1999**, *156*, 177−189.
(74) Ryan, B. J.; Poduska, K. M. Roughness Effects on Contact Angle Measurements. *Am. J. Phys.* **2008**, *76*, 1074−1077.
(75) Wang, C. L.; Zhou, B.; Tu, Y. S.; Duan, M. Y.; Xiu, P.; Li, J. Y.; Fang, H. P. Critical Dipole Length for the Wetting Transition Due to Collective Water-dipoles Interactions. *Sci. Rep.* **2012**, *2*, 358.
(76) Rafiee, J.; Mi, X.; Gullapalli, H.; Thomas, A. V.; Yavari, F.; Shi, Y. F.; Ajayan, P. M.; Koratkar, N. A. Wetting Transparency of Graphene. *Nat. Mater.* **2012**, *11*, 217−222.


DOI: 10.1021/acs.jpclett.8b00749
*J. Phys. Chem. Lett.* 2018, 9, 2346−2352

(77) Huang, D. M.; Geissler, P. L.; Chandler, D. Scaling of Hydrophobic Solvation Free Energies. *J. Phys. Chem. B* **2001**, *105*, 6704−6709.
(78) Hough, D. B.; White, L. R. The Calculation of Hamaker Constants from Liftshitz Theory with Applications to Wetting Phenomena. *Adv. Colloid Interface Sci.* **1980**, *14*, 3−41.
(79) Packham, D. E. Work of Adhesion: Contact Angles and Contact Mechanics. *Int. J. Adhes. Adhes.* **1996**, *16*, 121−128.
(80) Chandler, D. Interfaces and the Driving Force of Hydrophobic Assembly. *Nature* **2005**, *437*, 640−647.



DOI: 10.1021/acs.jpclett.8b00749
*J. Phys. Chem. Lett.* 2018, 9, 2346−2352